



Wireless Video Transmission and Control of Unmanned Surface Vehicle with Rudderless Double Thrusters

Dimitriy Georgiev, Richard Kaiva, Hou Yuan Ng,
Hristiyan Georgiev, Pedro Henrique, Rianne Drijver

supervised by
Dr. Ronald A.J. van Elburg

June 27, 2021

Abstract

The use of unmanned surface vehicles (USVs) for inspection of concrete structures is affected negatively by many external factors. Navigating a USV requires constant visual feedback of the vessel. The original setup of the studied USV (The HyDrone) has a limited video transmission range which does not allow for extended distance operations. Additionally, inspection work of concrete structures requires video footage from an underwater sonar camera, which can obtain high quality footage only when the USV moves parallel to the structures of interests with a controlled speed. This document presents an analogue video transmission device, enhancing the navigation process and aiding USV operators. A control-system, utilizing two time-of-flight sensors, an IMU, and a microcontroller was also developed to correct the orientation of the vehicle during inspection. Series of test were performed to evaluate the performance and demonstrate the practical value of the developed systems for wireless video transmission and control of unmanned surface vehicles.

Contents

1	Introduction	3
2	HyDrone	3
3	Methods	4
3.1	Video Transmission	4
3.1.1	Materials	5
3.1.2	Enclosure Design	6
3.1.3	Camera Placement	7
3.2	Control System	7
3.2.1	Materials and Sensors	7
3.2.2	Decoding RC signals	8
3.2.3	Modelling	9
3.2.4	Wall Following	10
4	Results	10
5	Discussion	15
6	Conclusions and Future Work	16

1 Introduction

Unmanned surface vehicles (USVs) have been playing an increasingly significant role in the field of naval operations, oceanography, mapping and inspection of aquatic environments.[1, 2] In fact, inspection of bridges and canal walls, below or above the water line, is the main business activity of *oQuay*. They conduct inspection of concrete structures in different ways, but one of their key instruments is an underwater sonar camera attached to a USV, called the HyDrone. In order to make video recordings of high quality it is essential to sail the HyDrone at a constant distance, parallel to canal walls. During operation, the position of the vehicle is affected by wind and water currents, making the sonar images blurry. The lack of a control system to correct the HyDrone's orientation is a pitfall in the design and affects the quality of the inspection work. Moreover, the current navigation system of the HyDrone, consisting of a GoPro camera, has a short transmission range of 10 meters. This imposes significant limitations on the operation of the vehicle and reduces the effective sailing range of the HyDrone. *oQuay* are looking for a system that can guarantee control of the movement of the vehicle and a device that can increase the transmission range of the video signal. This report introduces solutions to these problems. Section 3.1 details the design of a low-cost wireless video transmission device. Section 3.2 then describes the development of a control system for correction of the heading of the HyDrone. The experimental results are presented in Section 4. Sections 5 and 6 discuss some of the challenges faced in the presented solutions and attempt to describe the problems that still have to be addressed in order to make the control system functional. Finally, the appendix provides a link to the project page where all the necessary software and assembly files are available.

2 HyDrone

The HyDrone is a radio-controlled boat, shown in Figure 1, designed for hydrographic survey applications.[3] It has a double hull configuration and a custom propulsion system, consisting of two propellers driven by brushless DC motors. The catamaran structure prevents roll and pitch motions and maintains the position of the vessel balanced, while also improving manoeuvrability. The speed of the brushless motors is controlled by electronic speed controllers (ESCs) located inside each of the hulls. The ESCs are connected to 2.4 GHz radio receivers that interpret control commands sent from a human operator via a 2.4 GHz radio transmitter. The physical characteristics

of the HyDrone are shown in Table 1.



Figure 1: Seafloor Systems HyDrone USV

Table 1: Physical characteristics of the HyDrone

Parameter	Value
Length Overall (LOA)	1.16 m
Beam Overall (BOA)	0.73 m
Mass	9.8 kg
USV Velocity (max)	1.7 m/s
Payload (max)	15 kg

3 Methods

3.1 Video Transmission

A video transmission device is required in remote operation when inspection is carried out without clear visibility of the vehicle. Such a device can provide critical visual feedback to the operator of the vehicle, aiding in the navigation process. Analogue wireless, digital wireless, and digital wired are

the main types of technologies that can be utilized to implement a video transmission device. Wired solutions would impose limitations on the operation of the HyDrone and are therefore inconvenient for this application. Digital wireless solutions are popular due to their reliability and quality of video signal. However, in order to achieve low latency, digital solutions require processing units capable of implementing sophisticated transmission links and having high processing power to encode/decode video streams. Digital systems are significantly more expensive as a result. Analogue systems, on the other hand, transmit video by simply modulating the source signal onto a carrier frequency which makes them simple to implement and cheap to manufacture.

3.1.1 Materials

Most video transmission devices consist mainly of three separate components: a video transmitter (VTX), a video receiver (VRX), and a camera. The implementation of an analogue video transmission system for the HyDrone was based on first-person view (FPV) equipment due to the raising popularity and availability. A dedicated FPV camera can provide low latency video signal with standard definition, DVD-equivalent quality. The *RunCam Swift 2* with 1/3" CCD sensor and 2.3mm lens was chosen for its native 4:3 aspect ratio and resulting 140°-150° field-of-view (FOV). This configuration matched the aspect ratio of *oQuay*'s monitors and provided FOV similar to the GoPro camera.

The *Eachine TX805* was used as a VTX to transmit the video signal over 5.8GHz. The high transmission frequency allowed for use of small size antennas and limited interference from Wi-Fi signals, predominantly operating at 2.4GHz. The output power of the VTX was increased from 25mW to 200mW in order to increase the effective range of transmission. On the other hand, there were not significant considerations to be made in terms of video receiver. Most VRXs typically operate in the 5.8GHz range and support multiple bands and channels for signal reception. The *Eachine RC832* was selected based on positive reviews from the FPV community.

The last crucial part of the wireless system included selection of antennas that would be used on the transmitter and receiver end. Antennas are the deciding factor that determines the signal strength and range. For this reason, the stock dipole, linear polarized antennas that came with the VTX and VRX were replaced with circular polarized ones with +5dBi gain. Circular polarized antennas are known to reduce multipath interference and improve overall reception. The *Realacc* omni-directional, cloverleaf antennas with RP-SMA connectors were chosen to match with the antenna connectors on

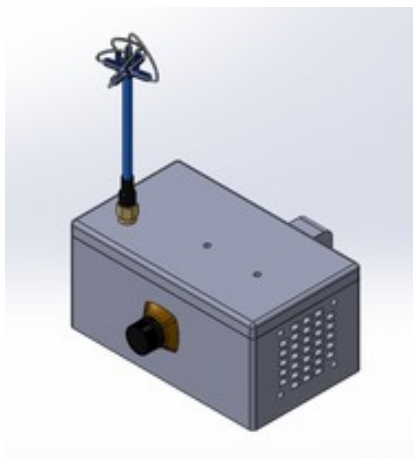
the receiver and transmitter.

Additionally, a RCA to HDMI converter was needed at the last stage of reception to convert the analogue signal, output from the VRX, to digital one that can be visualized by *oQuay*'s monitors.

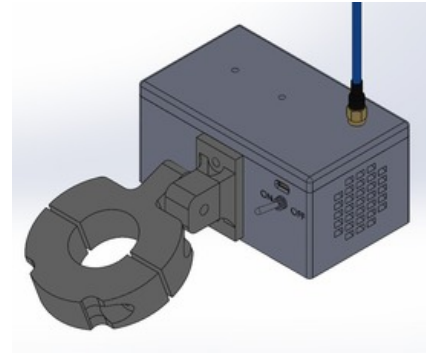
Finally, a Li-ion 18650 protected cell and a 1S-battery charging circuit were received from NKON, Eindhoven, the Netherlands, in order to power the FPV setup and allow for easy re-charge. The FPV components were ordered from Banggood, Guangdong, China. Further details on the electric components can be found on the project page, linked in the Appendix A.

3.1.2 Enclosure Design

A custom enclosure was designed in SolidWorks for housing the electric components of the FPV system. The design was specifically tailored to the 3D models of FPV components. The 3D models were obtained from GrabCAD and used as a reference for choosing dimensions of the enclosure and creation of openings and mounting holes. Air intake and outlet vents were added to the shorter sides of the enclosure box at a 20° angle to prevent water from entering the inside. Furthermore, a 40x40mm 12V fan was placed inside the enclosure to facilitate air circulation and heat transfer. The fan was specifically included to reduce the likelihood of having the video transmitter overheat. Passive cooling was not sufficient to maintain operating temperature for the transmitter. The rendered model of the complete FPV system can be seen in Figures 2a and 2b. A technical drawing of the enclosure is also available in Appendix C. All of the parts can be reproduced in case of damage, based on the created drawings, available on the project page.



(a) Front view



(b) Rear view

3.1.3 Camera Placement

It was important to be able to adjust the camera angle based on the preferences of the operator of the vehicle. A fixture was designed to allow clamping the FPV system to a Ø 15mm metal rod, attached to the HyDrone. An adjustable hinge, fastened with a M5 countersunk bolt, allowed to point the camera lens at any desired vertical or horizontal direction. The position of the camera was chosen in a way to include both hulls of the platform in the video feed. This provides a good reference point for the operator when the boat is not in line of sight and the operator navigates solely based on the video stream.

3.2 Control System

A control system that can adjust the heading of the vehicle and maintain constant distance to walls is needed to improve the quality of inspection and ease the workload on the operator of the HyDrone. Open-loop, Closed-loop, Model Predictive, and Reinforcement learning are the main types of control methodologies that can be utilized to implement such a system. Open-loop control would not be sufficient in the environment of the HyDrone where disturbances of different sources are present. Model predictive control and reinforcement learning solutions require more development time and do not deliver necessary better results compared to closed-loop. Closed-loop control is intuitive and effective when implemented in the form of a PID regulator.

3.2.1 Materials and Sensors

On a hardware level, a closed-loop control system requires three main components: actuators that can change the state of the system, sensors that measure physical properties of the environment, and a microcontroller to process sensor information and send commands to the actuators. The HyDrone was already equipped with actuators in the form of underwater thrusters, but sensors and microcontroller were still to be added. Ranging sensors were necessary as the task required implementing wall-following behaviour. The ST VL53L1X Time-of-Flight (ToF) sensor was used to measure distance to walls. The ToF sensor was chosen over ultrasonic one due to increased sensing range and low sensitivity to external disturbances such as wind. Additionally, the TI TCA9548A 8-channel digital multiplexer was included to allow for expansion with multiple ToF sensors that have the same I2C address. The ST LSM6DS3 inertial measurement unit (IMU) was included in the setup to keep track of the heading of the vehicle during operation. The Arduino Nano

(ATmega328) was chosen as a microcontroller to implement the control logic and data acquisition of the system. Besides the microcontroller, a Raspberry Pi Zero W was used for data storage, over-the-air (OTA) programming, and communication with the GoPro camera of the HyDrone. The sensors and multiplexer were ordered from AliExpress, Hangzhou, China, while the microcontroller and Raspberry Pi were received from Kiwi Electronics, Den Haag, the Netherlands. The IMU and ToF sensors were calibrated according to the procedures in [4]. Finally, all of the electrical components of the control system were placed in a IP66 rated box for protection. A custom adaptor plate was designed for mounting the ToF sensors to the outside of the enclosure box at 45° and 90° to the side of the HyDrone, seen in Figure 3. Further details on electrical connections can be found in the schematic, provided in Appendix B.

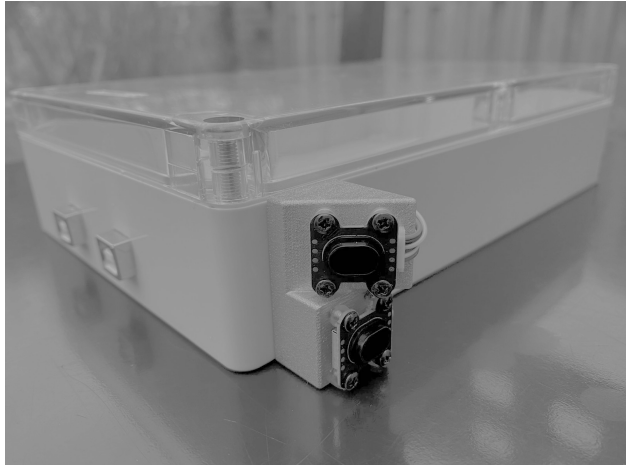


Figure 3: Mounted ranging sensors

3.2.2 Decoding RC signals

Before being able to implement any type of control, the microcontroller had to be installed and programmed to intercept the RC signals output of the radio receiver. The RC signals are PWM signals with varying pulse width from 1000 - 2000 μ s. A 1000 μ s pulse represents full throttle backwards, while a 2000 μ s pulse represents full throttle forwards, and 1500 μ s respectively being the idle state of an underwater thruster. In order to measure the pulse width with the microcontroller, the time between occurrence of rising and falling edge was recorded via Pin Change Interrupts. Pin Change Interrupts also improved firmware performance and reduced likelihood of data corruption.

tion. The 16 MHz clock on the Arduino Nano provided $4\mu s$ resolution, which was high enough to measure pulses' width.

3.2.3 Modelling

The propulsion system of the HyDrone has no rudder to adjust its heading, but instead a differential steering mechanism that requires two inputs, illustrated in Figure 4.

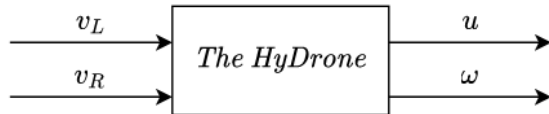


Figure 4: Block diagram of the propulsion system

where v_L and v_R are the two propeller speeds (left and right) in revolutions per second [rps], u is the linear velocity in meters per second [m/s] and ω the angular velocity of the vehicle in degrees per second [dps]. The linear and angular velocities for differential drive are defined as follows:

$$u = \frac{(v_L + v_R)}{2} \quad (1)$$

$$\omega = \frac{v_L - v_R}{2} \quad (2)$$

The orientation of the vehicle can be determined through integration of the angular velocity that is measured by the gyroscope of the IMU Integration in discrete time is approximated to:

$$\phi_n = \phi_{n-1} + \omega \Delta t \quad (3)$$

where ϕ_n is new orientation angle, ϕ_{n-1} is the previously recorder angle, and ω is the angular velocity sampled at regular time intervals.

Furthermore, the 3-DoF MEMS gyroscope that is part of the IMU can be modelled as a second-order process with dead-time (SOPDT), [5], according to the following equation:

$$\tau^2 \frac{\delta^2 y}{\delta \tau^2} + 2\zeta\tau \frac{\delta y}{\delta t} + y = K_p u(t - \theta) \quad (4)$$

where the output $y(t)$ and input $u(t)$ represent resulting angular velocity [dps] and step control signal [0-100] respectively. τ , ζ , K_p , and θ are the four unknown parameters that can be determined experimentally. The model

can later be used to test out parts of the control system in a simulated environment. The model can also be applied to check the stability of the designed controller.

3.2.4 Wall Following

The implemented wall following algorithm was based on trigonometric functions and the estimated orientation of the vehicle. The goal of the algorithm is to calculate an error in the orientation α which can then be used to adjust the speed of the thrusters in order to minimize it. The sketch for deriving a mathematical equation for calculation of the error α is seen in Figure 5. OP and D_{wall} are constants that can be tuned to adjust the behavior of the controller, i.e. make it more/less aggressive. The length of OA is the distance measured by the 90° ranging sensor.

$$\alpha = \beta - \theta$$

$$\beta = \tan^{-1}\left(\frac{CP}{OP}\right)$$

$$CP = OH - D_{wall}$$

$$OH = \cos \theta \cdot OA$$

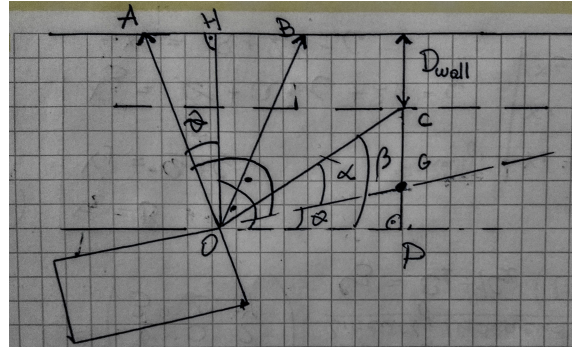


Figure 5: Wall following algorithm sketch

4 Results

FPV

The assembled version of the FPV system is shown in Figure 6.



Figure 6: Assembled video transmission device

One of the first tests aimed to determine whether the power input to the video transmitter was influenced by voltage ripple which could be negatively contributing to glitch effect in the received video. The system was powered by a single battery cell whose voltage was increased through a boost-converter to 12V. An oscilloscope was used to measure the voltage ripple output from the power circuit seen in Figure 7.



Figure 7: Oscilloscope snapshot, 1.30V p-p ripple

The mean peak-to-peak value of 1.30V ripple was not significant to cause signal loss, but its' presence was undesirable. A $330 \mu F$ low ESR capacitor was then added to the circuit to reduce the voltage ripple. This resulted in 50% reduction of the amplitude of the ripple, as seen in Figure 8.

Another test was performed to verify the ability of the FPV system to



Figure 8: Oscilloscope snapshot, 0.648V p-p ripple

maintain near ambient temperature inside the enclosure. An NTC thermistor was mounted onto the transmitter and temperature readings were recorded every 30 seconds over 5 minute interval. It can be seen from the results, Figure 9, that the internal temperature rises significantly more when the fan is turned off.

Table 2: Internal Temperature of FPV system

Time [s]	ADC Value (Fan OFF)	ADC Value (Fan ON)
0	489	502
30	506	502
60	529	508
90	545	514
120	553	518
150	569	521
180	581	524
210	590	526
240	600	526
270	607	526
300	613	527

To verify the client's range requirement of at least 100 meters, a clear line-of-sight test was carried out with the FPV setup. Obstacles such as walls and glass windows had to be avoided, that is why the experiment was conducted outside the school building. Due to lack of mains power outside, a 12V compatible monitor was used to observe the video stream. A 12V car battery was used to power the test setup. To mimic the normal working conditions, the antenna of the receiver was placed upright to maintain the alignment with the transmitting antenna on the camera enclosure. The fully

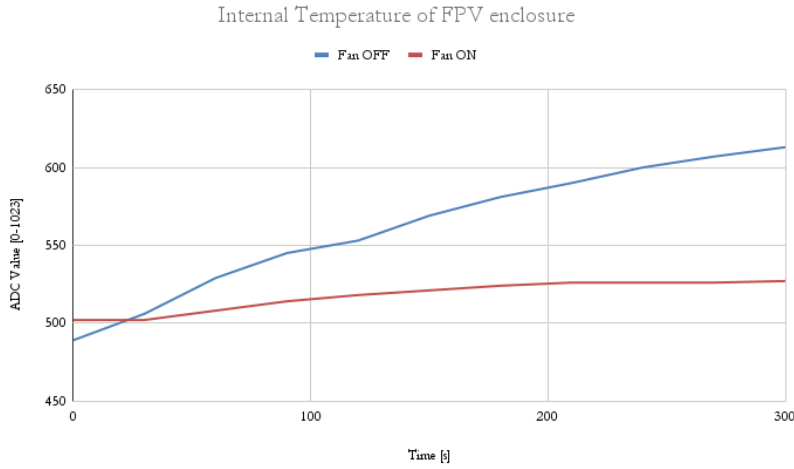


Figure 9

charged transmitting counterpart of the system was switched on and moved away from the receiver in steps of 10 meters. A GPS sensor was used to record the movement of the camera allowing to reconstruct the travelled path and calculate the effective range. The result is illustrated in Figure 10 Upon the completion of every distance interval, the quality of the video stream was evaluated by two team members based on a three point scale (bad, fair, good). Additionally, notes were taken to further characterize the clarity of the video stream and GPS coordinates were recorded as seen in Table 3.



Figure 10: FPV range test - 500m

Clear line-of-sight Test					
Distance	Quality	Notes	Start Coordinates	End Coordinates	
0 - 200	good	Image gliching a few times (once every 2 min)	52°59'57.4"N 6°34'14.2"E	52°59'58.7"N 6°34'23.4"E	
200 - 400	fair	Gliching increases (twice every minute) but image is still fine for navigation, stability of the camera reduces gliches	52°59'58.7"N 6°34'23.4"E	53°00'00.6"N 6°34'34.7"E	
400 - 500	bad	Glich increases (around once every 3 sec), quality is bad but if really needed navigation can happen with some effort	53°00'00.6"N 6°34'34.7"E	53°00'02.5"N 6°34'41.1"E	
>500	bad	Gliche increases depending on obstacles and stability	-	-	

Table 3: Notes and GPS coordinates during FPV range test

HyDrone Control

The validation phase of the control system was limited and insufficient to resolve problems around it. The current state of the system does not allow moving the vehicle parallel to canal walls. The moment the control system is turned on, the vehicle begins rotating to adjusts its' heading but then over-shoots the setpoint. Regardless, data was collected about the step response of the gyroscope in order to find the unknown parameters in Equation 4. The determined parameters can be seen in Table 4 and the modelled step response in Figure 11.

Table 4: SOPDT model parameters

Parameter	Value
K_p	2.26
τ	0.17
θ	-0.03
ζ	0.72

where K_p is process gain, τ is time constant (normalized 0-1), θ is dead-time (normalized 0-1), ζ is damping ratio.

It was noticed during testing that the gyroscope experienced voltage spikes outside expected range, illustrated in Figure 12a. It was necessary to implement a digital filter that can suppress those spikes. The HyDrone moves slowly with a maximum velocity of 1.7m/s, therefore the cutoff frequency of the filter can be set quite low. A low-pass filter in the form of an IIR filter with cutoff frequency of 3 Hz was added. This resulted in clearing the unexpected values, as seen in Figure 12b. A similar filter was added to the measurement of the ToF sensors as well.

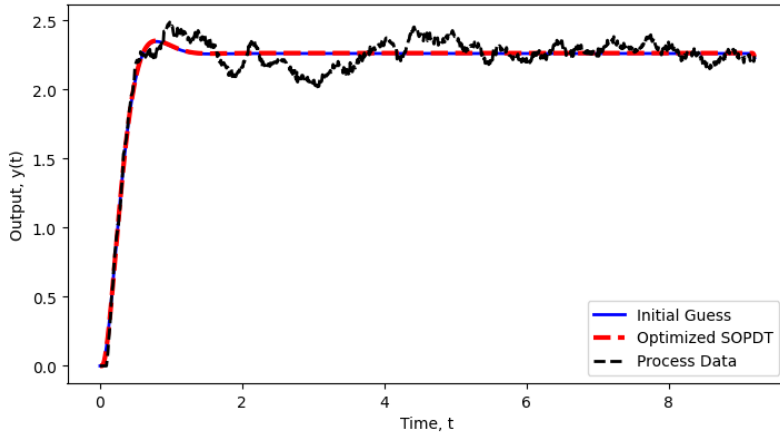


Figure 11: Optimization fit of second-order model to raw gyro data

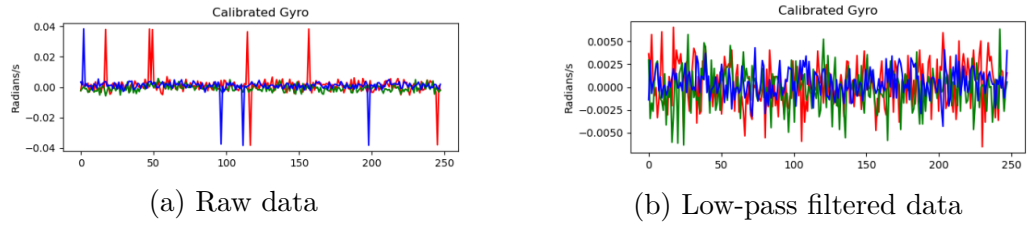


Figure 12: Observations on gyroscope data

5 Discussion

The FPV system is complete and ready for exploitation. On the other hand, the control system requires further testing and debugging before it can be delivered to a customer. One of the mistakes that was repeatedly made until now was to test the control system together with the HyDrone. Debugging the complete setup is difficult and time consuming. That is why, it is necessary to test isolated parts of the system first. The control box can be detached from the HyDrone and placed, for example, on a 4-wheel trolley cart to see how the sensors respond when the trolley is moved alongside a wall. In this way, one can easily determine and record the input/output of the implemented control laws and allow to understand how the system responds.

Furthermore, the authors of [6] propose a methodology for modelling of a USV with rudderless double thrusters that can be applied in this situation as well. The established 3-DoF dynamic model and propeller thrust model enables accurate approximation of the state of the vessel in any point of time.

The availability of an accurate USV model of the HyDrone would allow to work in a simulated environment which is imperative to any effective control design.[7]

6 Conclusions and Future Work

A video transmission device and a control system for an unmanned surface vehicle were developed to aid inspection work of concrete structures. More specifically, the transmission device can be used to provide visual feedback to human operators, while the control system can correct the heading of the vessel in order to sail at a constant distance to walls. The video device was built with off-the-shelf FPV components and achieves wireless analogue transmission with a range exceeding 100 meters. The analogue nature of the transmitted signal results in noticeable glitch effect in the video feed when the device moves further than 200 meters from the receiver. Regardless, the results meet client requirements and the device is considered well-designed with a budget of €100.

The designed control system has the potential of sailing an USV parallel to canal walls, however, the system is still under development. Moreover, it requires further testing and tuning of parameters in order to achieve the desired behavior. For this purpose, it is essential to establish a model about the kinematics and perhaps even kinetics of the USV in order to realize intelligent control and maneuverability prediction of the vessel.

Reinforcement Learning

A different approach based on machine learning can also be applied in an attempt to solve the control task. The process of fine-tuning low-level parameters in order to achieve a particular control task is often iterative and prone to programmer bias. For this reason, the idea of providing high-level specifications and allowing computers to learn from empirical observations of the world is appealing. In the context of reinforcement learning, the environment in which the vehicle operates can be described by a set of states. The vehicle can be represented as an agent that can take one out of a fixed number of actions at each point of time. After choosing an action, the agent receives a reward, which reflect how good the action was. Ultimately, a reinforcement learning algorithm aims to come up with an optimal value function which is capable of mapping states (or states and actions) to a measure of long-term value for being in that state.[8] During operation, it can be assumed that the HyDrone begins along-side a canal wall with a pre-

defined desired distance. The desired distance can be denoted with D_{wall} and set to 0.8 meters. The vehicle can be considered to be in the desired position if it does not exceed ϵ_{wall} distance from D_{wall} . The 45° and 90° ranging sensors define two distinct regions in which measurement can be categorized in three states:

$$state(d) = \begin{cases} \text{Too Close} & \text{if } d < D_{wall} - \epsilon_w \\ \text{Good} & \text{if } (D_{wall} - \epsilon_w) \geq d \geq (D_{wall} + \epsilon_w) \\ \text{Too Far} & \text{if } d > D_{wall} + \epsilon_w \end{cases} \quad (5)$$

The total number of states is equal to the number of combinations for each region, hence $3^2 = 9$. Assuming that the sensors are sample at 100 Hz the time step to update the state will be $\frac{1}{100}$ of a second.

The movement of the HyDrone is controlled by the speed of the underwater thrusters which is regulated by the PWM signal sent from the microcontroller. The vehicle can be assumed to perform only three distinct actions - move left, right, and forward. This creates a layer of abstraction from the low-level parameters and PWM signal, and would require to program a type of translation mechanism. Additionally, it is important that the move left and move right actions have a small forward component in them, in order to prevent the vehicle from getting stuck in oscillatory movement.

The reward function for the reinforcement learning algorithm can be designed as:

$$reward(s_t, a_t) = \begin{cases} -10 & \text{if not moving OR hit wall} \\ -1 & \text{if } state = \text{Too Close OR Too Far} \\ 2 & \text{if } state = \text{Good AND action} = \text{Forward} \\ 0.5 & \text{if } state = \text{Good} \end{cases} \quad (6)$$

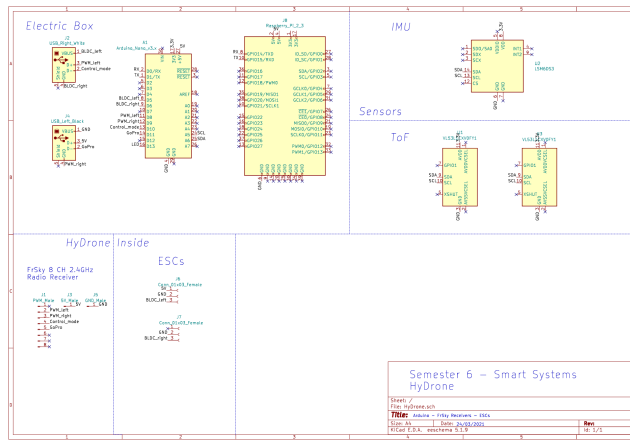
which implies that maximum reward is returned if the HyDrone stays within the desired state and executes the move forward action. Sanctions, or negative rewards, are necessary for undesirable events, such as the vehicle staying at rest or hitting the canal wall.

Appendix

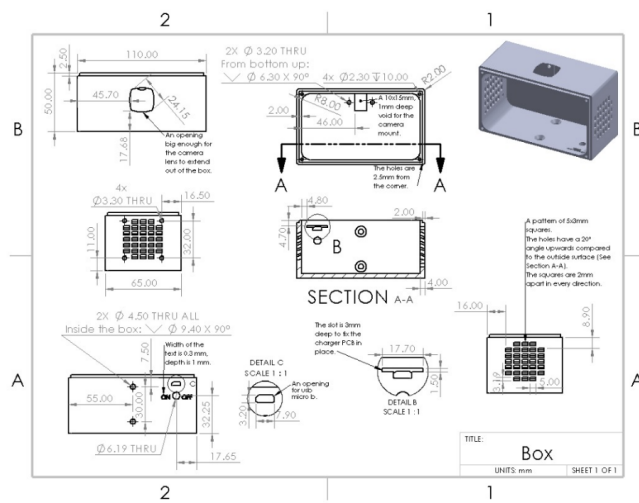
A. Software and Assembly Files

The project files are available on GitHub:
<https://github.com/Silverlined/HyDrone-Control-System>

B. Electrical Schematic



C. CAD Drawings



References

- [1] Ru-Jian Yan et al. “Development and missions of unmanned surface vehicle”. In: *Journal of Marine Science and Application* 9.4 (2010), pp. 451–457. DOI: 10.1007/s11804-010-1033-2.
- [2] Justin E. Manley. “Unmanned surface vehicles, 15 years of development”. In: *Oceans* (2008). DOI: 10.1109/oceans.2008.5289429.
- [3] oQuay. *Design History File: Q-001*.
- [4] Dimitriy Georgiev. *Design History File: Procedures*.
- [5] *Dynamics and Control*. URL: <https://apmonitor.com/pdc/index.php/Main/SecondOrderOptimization>.
- [6] Chunyue Li et al. “Modeling and Experimental Testing of an Unmanned Surface Vehicle with Rudderless Double Thrusters”. In: *Sensors* 19.9 (2019). ISSN: 1424-8220. DOI: 10.3390/s19092051. URL: <https://www.mdpi.com/1424-8220/19/9/2051>.
- [7] Onny Sutresman, Rafiuddin Syam, and Sapta Asmal. “Controlling Unmanned Surface Vehicle Rocket using GPS Tracking Method”. In: *International Journal of Technology* 8.4 (2017). ISSN: 2087-2100. URL: <http://ijtech.eng.ui.ac.id/old/index.php/journal/article/view/9481>.
- [8] W.d. Smart and L. Pack Kaelbling. “Effective reinforcement learning for mobile robots”. In: *Proceedings 2002 IEEE International Conference on Robotics and Automation (Cat. No.02CH37292)* (). DOI: 10.1109/robot.2002.1014237.